Original scientific paper

Potential of imaging analysis in establishing skin concentration-distance profiles for topically applied FITC-dextran 4 kDa

Shosho Kijima[1], Ryosuke Masaki[1], Wesam R. Kadhum[1], Hiroaki Todo[1], Tomomi Hatanaka[2], Kenji Sugibayashi[1,✉]

[1] *Faculty of Pharmaceutical Sciences, Josai University, 1-1 Keyakidai, Sakado, Saitama 350-0295, Japan*
[2] *Institute of Innovative Science and Technology, Medical Science Division, Tokai University, 4-1-1 Kitakaname, Hiratsuka, Kanagawa 259-1292, Japan*

✉Corresponding Author: E-mail: sugib@josai.ac.jp; Tel.: 049-271-7367; Fax: 049-271-8137

Abstract

Quantitatively determining the skin concentration-distance profiles of topically applied drugs is important for evaluating their safety and efficacy. The aim of the present study was to quantitatively visualize the distribution of hydrophilic drugs through the skin using confocal laser scanning microscopy (CLSM) in order to obtain skin concentration-distance profiles. FITC-dextran with a molecular weight of approximately 4 kDa (FD-4) was selected as the model fluorescent drug in the present study, and excised pig ear skin was used. The skin concentration of FD-4 at each depth of a skin section was assessed by imaging analysis of the intensity of fluorescence. The FD-4 skin concentration-distance profile obtained was analyzed using Fick's second law of diffusion, and was markedly similar to that using skin permeation parameters in the skin permeation study. These results suggest that the present CLSM method may be a promising tool for quantitatively visualizing the concentration-distance profiles of drugs through the skin.

Keywords

Confocal microscopy; FITC-dextran, dermatopharmacokinetics, skin permeation

Introduction

Drug delivery through the skin remains an attractive and challenging area for research and development. Most of the drugs contained in transdermal delivery systems are lipophilic with low molecular weights. However, various chemical and physical approaches have been used to overcome the barrier function of the stratum corneum so that even malabsorptive hydrophilic and high weight molecular compounds can diffuse into the deeper regions of the skin. An assessment of the chemical concentrations of drugs in the skin is essential for developing topical pharmaceutical products and functional cosmetics; therefore, drug disposition in the skin (stratum corneum, viable epidermis/dermis, and appendages) as well as the concentration-distance profiles of these compounds through the skin need to be elucidated in more detail [1-4].

Since the skin, which is a structurally heterogeneous organ, is not uniformly distributed for topically applied drugs, it remains unclear how drugs permeate the skin layers from the surface to deeper regions

over time. The skin is an extremely thin organ; thus, as a small amount of a drug may result in a high target concentration, a sensitive method is needed to determine the drug concentration in each layer of the skin after its topical application.

Several conventional methods, including the suction blister [5], punch and shave biopsy [6], and homogenization [7] methods, have been used to measure the concentration of a drug in the skin. However, these methods can only measure average drug concentrations in the total area of excised whole skin instead of those at each depth of the skin. Furthermore, these methods cannot provide a visual observation of drug disposition from the surface to deeper regions of the skin, which is necessary for further understanding of the dermatopharmacokinetics of topically applied drugs. The tape-stripping method [8-12] has been used to measure drug concentrations at each depth of the skin, but only in the stratum corneum. A clearer understanding of drug disposition through the whole skin will be helpful for evaluating their safety and efficacy by specifying the skin tissue targeted by these drugs.

However, the drug concentration at each depth of the skin has been predicted using various mathematical equations [13-18]. We previously reported that the cutaneous disposition of topically applied drugs could be predicted using the difference method based on Fick's 2nd law of diffusion, and also that the average drug concentration in the stratum corneum and viable epidermis/dermis could be determined separately [19-22]. However, Fick's law-based approach requires a relatively advanced knowledge of mathematical equations in order to estimate the cutaneous disposition of topically applied drugs.
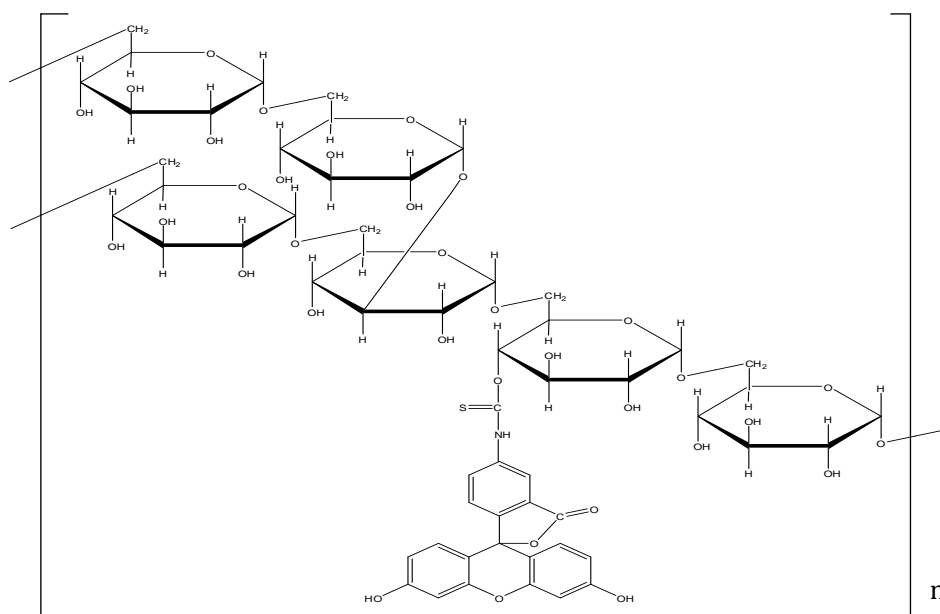

Figure 1. Chemical structure of FD-4

Therefore, the aim of the present study was to develop a quantitative, visual, simple, sensitive, and effective method to analysis concentration-distance profile of topically applied compounds using confocal laser scanning microscopy (CLSM). The CLSM could be used to quantitatively visualize disposition of fluorescent compounds or high molecular weight compounds with fluorescent labeling moiety through the skin from the viewpoint of depth. In the present study, the mathematical approach represented by the difference equation method based on Fick's law of diffusion to obtain a concentration-distance profile was also used for comparisons to the CLSM technique. We applied FITC-dextran (Fig. 1) having a molecular

weight of about 4 kDa (FD-4) as a candidate to excised skin from the pig ear in which the stratum corneum had been removed by stripping. Dermatodynamics could be closely related to drug concentration in viable epidermis and dermis not in the stratum corneum after topical application. Thus, we selected the stripped skin to investigate the possibility of quantitative determination of FD-4 concentration in viable epidermis and dermis. Concentration-distance profile of FD-4 through the skin was quantified by imaging analysis (CLSM) over time.

Theoretical [22-25]

Stripped skin excised from the pig ear was assumed to be a homogeneous membrane [26]. The present chemical compound permeation study through the skin was performed at an infinite dose under a sink condition in the receiver compartment. Figure 2 illustrates the typical concentration-distance profile of a chemical compound across stripped skin in the present study.
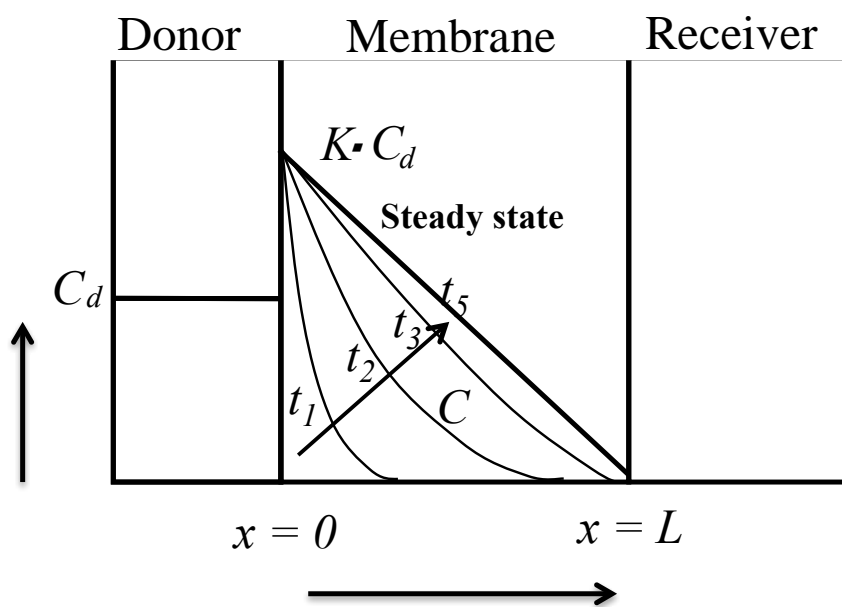
Figure 2. Schematic diagram of a concentration-distance profile in stripped pig ear skin (one-layered diffusion model)

The concentration of the chemical compound, C_s, in the stripped skin at a position, x, and time, t, was expressed by Fick's 2nd law of diffusion as follows:

$$\frac{\partial C_S}{\partial t} = D_S \frac{\partial^2 C_S}{\partial x^2} \tag{1}$$

where D_s is the effective diffusion coefficient of the chemical compound in the stripped skin. The initial condition (I.C.) and boundary condition (B.C.) in the present study were as follows:

I.C. $t = 0$ $0 < x < L$ $C_s = 0$

B.C. $t > 0$ $x = 0$ $C_s = KC_v$

          $x = L$ $C_s = 0$

$$V_d \frac{dC_d}{dt} = AD_S \frac{dC_S}{dx} \tag{2}$$

where L is the thickness of the stripped pig ear skin (1000 μm), K is the partition coefficient of the chemical compound from the donor solution to the stripped skin, C_v is the chemical compound concentration in the donor solution, V_d is the volume of the donor solution, and A is the effective permeation area of the skin.

The left and right members in Eq. (1) can be expressed by the following difference formulations [27]:

$$\frac{dC_{i,j}}{dt} = \frac{1}{\Delta t}\left(C_{i,j+1} - C_{i,j}\right) \tag{3}$$

$$D_S \frac{d^2 C_{i,j}}{dx^2} = \frac{D_S}{\Delta x^2}\left(C_{i-1,j} - 2C_{i,j} + C_{i+1,j}\right) \tag{4}$$

where C_{ij} is the concentration of the chemical compound at the i-th position and j-th time. Δx is x_i+1-x_i and Δt is t_j+1-t_j. By substituting Eqs.(3) and (4) into Eq. (1), the following equation was obtained.

$$C_{S_{i,j+1}} = rD_S C_{S_{i-1,j}} + \left(1 - 2rD_S\right)C_{S_{i,j}} + rD_S C_{S_{i+1,j}} \tag{5}$$

where r shows $\Delta t/\Delta x^2$.

The concentration of FD-4 in the stripped pig ear skin was obtained by a curve fitting the cumulative amount of FD-4 that permeated through the stripped skin to the theoretical values using a least squares method. The least squares calculation was performed using the spreadsheet software Microsoft® Excel and Δt and Δx were set where $D_s r$ may become 0.5 or less.

Experimental

Materials and methods

FD-4 was obtained from Sigma-Aldrich (St. Louis, MO, U.S.A.). The cellophane tape (Packaging tape, Series 405) used for tape stripping was obtained from Nichiban Co., Ltd. (Tokyo, Japan). Other reagents and solvents were of reagent or HPLC grade and used without further purification.

Experimental animals

The edible ears of three yuan pigs were obtained from Saitama Experimental Animals[*] (Sugito, Saitama, Japan). Animal experiments were approved by the Institutional Animal Care and Use Committee of Josai University (Sakado, Saitama, Japan).

Skin extraction and pretreatment

The skin used in the FD-4 permeation experiment was carefully washed and wiped well with distilled water, and the surface of the stratum corneum surface was tape-stripped 50 times using cellophane tape to remove the whole layer of the stratum corneum. One thousand-micrometer-thick stripped pig ear skin slices were prepared using a dermatome (Acculan 3Ti Dermatome, Aesculap-a B. Braun Company, Melsungen, Hessen, Germany) to separate the upper epidermis from the dermis and subcutaneous tissues [28].

---

[*] Now, all the business was entrusted to the Tokyo Laboratory Animals (Tokyo, Japan).

*Preparation of pig ear skin pieces for the calibration of FD-4 concentrations*

To prepare a calibration curve for the quantitative analysis of FD-4, excised stripped pig ear skin pieces were cut into an appropriate size and completely immersed in solutions with different concentrations of FD-4 (0.05, 0.50, 1.00, 2.50, 4.00, and 5.00 mM). As a control, skin pieces were immersed into pH 7.4 phosphate-buffered saline (PBS). All skin pieces were removed after 24 hours, embedded in super cryoembedding medium (Section-Lab, Hiroshima, Japan), frozen in isopentane cooled with dry ice to -20 °C, and then stored at -30 °C before further use.

Skin section observations using a confocal laser scanning microscope (CLSM)

Ten-micrometer-thick skin sections were prepared in a vertical direction by a cryostat (CM3050, LEICA, Wetzler, Hessen, Germany) using the skin pieces obtained as described in (3.4). The intensity of fluorescence was observed in these skin sections by CLSM (Fluoview FV1000 and software: FV10-ASW, Olympus, Tokyo, Japan). The CLSM conditions for FD-4 were as follows: wavelength, 473 nm; scan speed, 200 μs/pix; laser power, 1 %; high voltage, 236 V; gain, 1.125 x; and offset, 0.

Calculation of fluorescence intensity for FD-4 from CLSM images

Analysis points (50 points) were selected to calculate the fluorescence intensity for FD-4 from one skin section, and an average value was obtained from these points. Figure 3 shows an exemplified plot. The intensity of autofluorescence was obtained separately from an image of a skin section immersed in PBS alone and was then used to determine the actual fluorescence intensity for each concentration of FD-4.
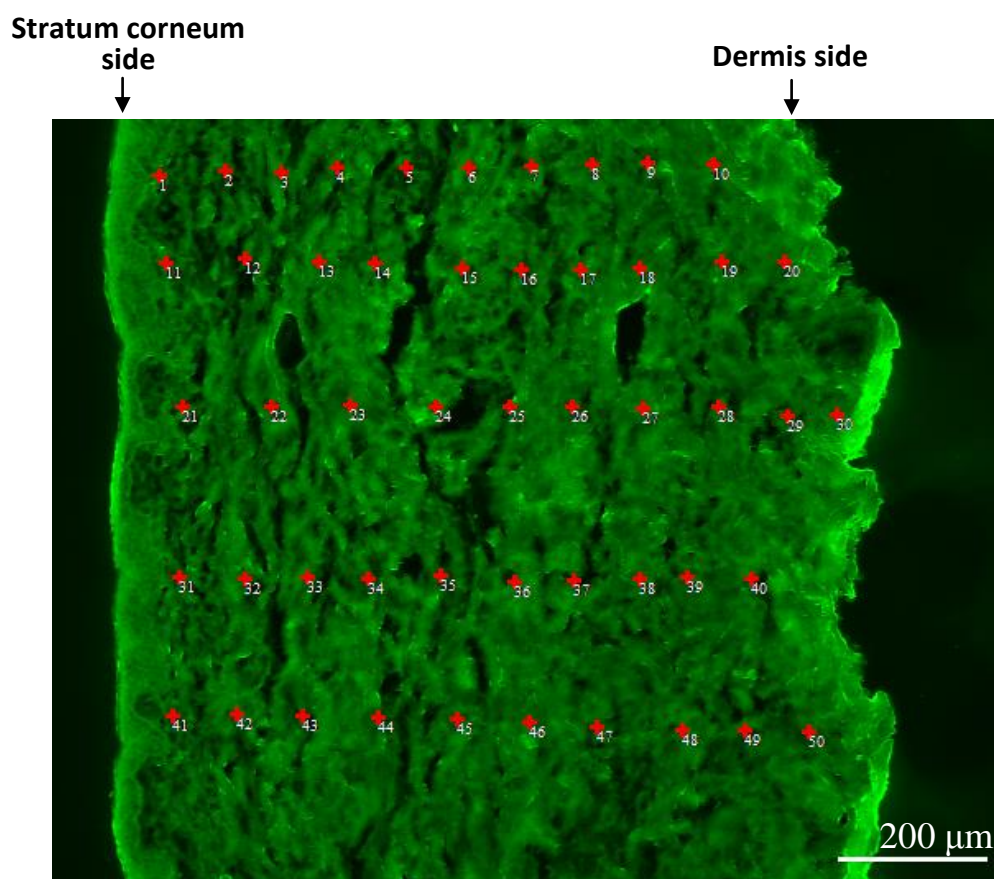
Figure 3. Example of a CLSM observation image for the calibration of FD-4 fluorescence intensity in stripped pig ear skin

Skin permeation experiments for FD-4

Stripped skin samples were set in vertical-typed diffusion cells (effective diffusion area: 1.77 cm^2) with the epidermis side facing the donor compartment. PBS (pH 7.4, 1 and 6 mL) was applied to the donor and receiver cells, respectively, for 1 h prior to starting the skin permeation experiment in order not only to reduce the influence of autofluorescence leaking into the receiver side, but also to hydrate the skin. After recovering PBS from the epidermis side, the same volume of 5 mM FD-4 was added to start the permeation experiment. Skin permeation experiments were performed at 32 °C over 5 h, and the receiver solution was continuously stirred with a star-head-type magnetic stirrer. At the predetermined times, an aliquot (0.5 mL) was withdrawn from the receiver cell and the same volume of PBS was added to the compartment to keep the volume constant. The concentration of FD-4 in the sample was measured by a fluorescence spectrophotometer (RF-5300, Shimadzu Corporation, Kyoto, Japan).

Determination of FD-4

The sample solution of FD-4 obtained from the permeation experiment was centrifuged (18,800 ×g, 4 ˚C, 5 min) and 300 μL of the supernatant was used for determination at excised and fluorescence wavelengths of 490 and 520 nm, respectively.

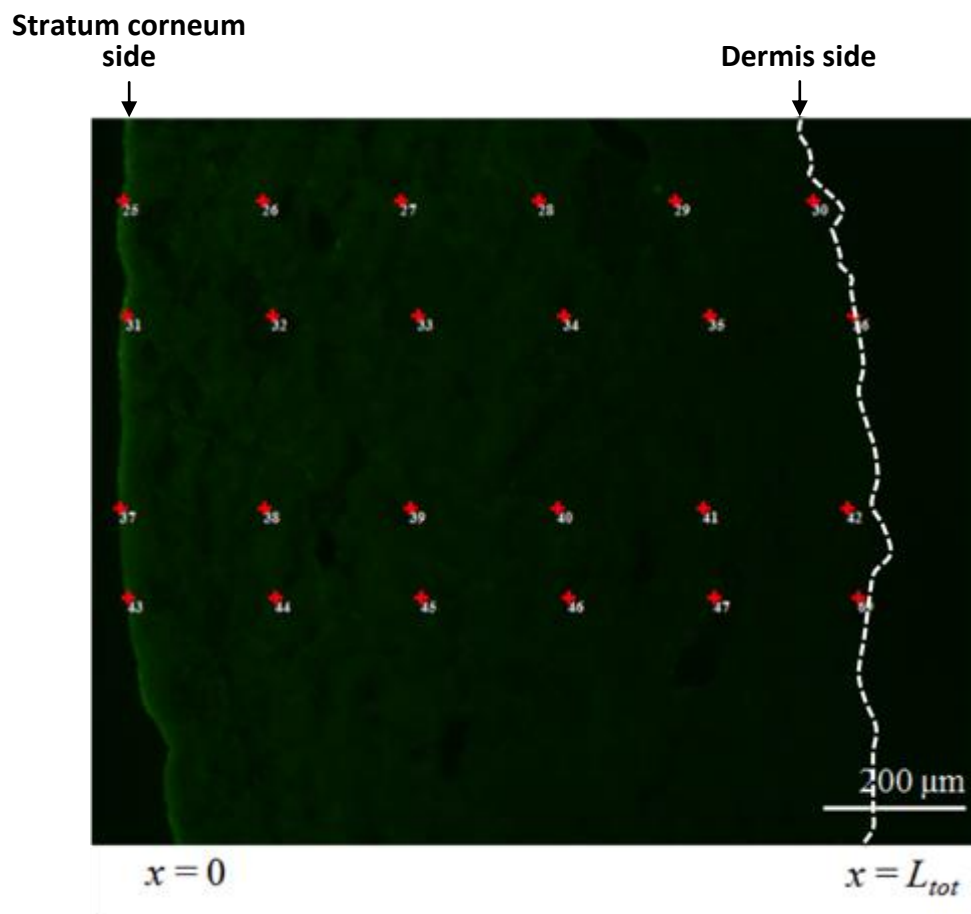*Skin treatment after the skin permeation experiment for FD-4*

Skin sectioning was only performed after the permeation experiment for FD-4. After the permeation experiment, the skin surface was washed three times using 1 mL of PBS on the Franz-type diffusion cell. The skin sample taken from the diffusion cell was cut vertically using a razor blade, embedded in super cryoembedding medium, and frozen in isopentane cooled with dry ice. Skin slices (10 μm in thickness) were made using a cryostat and observed under CLSM. The CLSM conditions have already been described above.

Image analysis of skin sections using CLSM

Skin section images were obtained by CLSM. Six points under one line were plotted from the epidermis side (x = 0) onto these images to calculate the fluorescence intensity. Four lines were then measured to determine the intensity of fluorescence. The average intensity of fluorescence was calculated from the same depth position of the plot. Figure 4 shows a plotting example. The average fluorescence value at each depth was obtained by subtracting the average autofluorescence values.

Analysis of statistics

The calibration curve for the concentration of FD-4 in skin sections using CLSM was analyzed by Pearson's correlation coefficient (R2) to determine whether a linear relationship existed between the intensity of fluorescence and concentration of FD-4 in the skin sections.

Figure 4. Example of a CLSM observation image for FD-4 fluorescence intensity in stripped pig ear skin after the permeation experiment. Dashed line: boundary of the skin

Results

CLSM observations of pig ear skin sections immersed in solutions with various concentrations of FD-4

Stripped pig ear skin was observed by CLSM after the application of solutions with different concentrations of FD-4. Figure 5 shows CLSM images of pig ear skin sections after their immersion in solutions with various concentrations of FD-4. Figure 5g shows the control (the immersed concentration of FD-4 is 0). Elevations were observed in the intensity of fluorescence in the image with increases in the immersed concentration of FD-4 (Fig. 5a→f).

Calibration curve of FD-4 in skin sections observed by CLSM

Figure 6 shows a calibration curve of the average intensity of fluorescence due to FD-4 in stripped skin as obtained from CLSM images (Fig. 5). A strong correlation (R^2=0.99636) was observed between the intensity of fluorescence in the skin and concentration of FD-4 applied.

Stratum corneum side

Dermis side
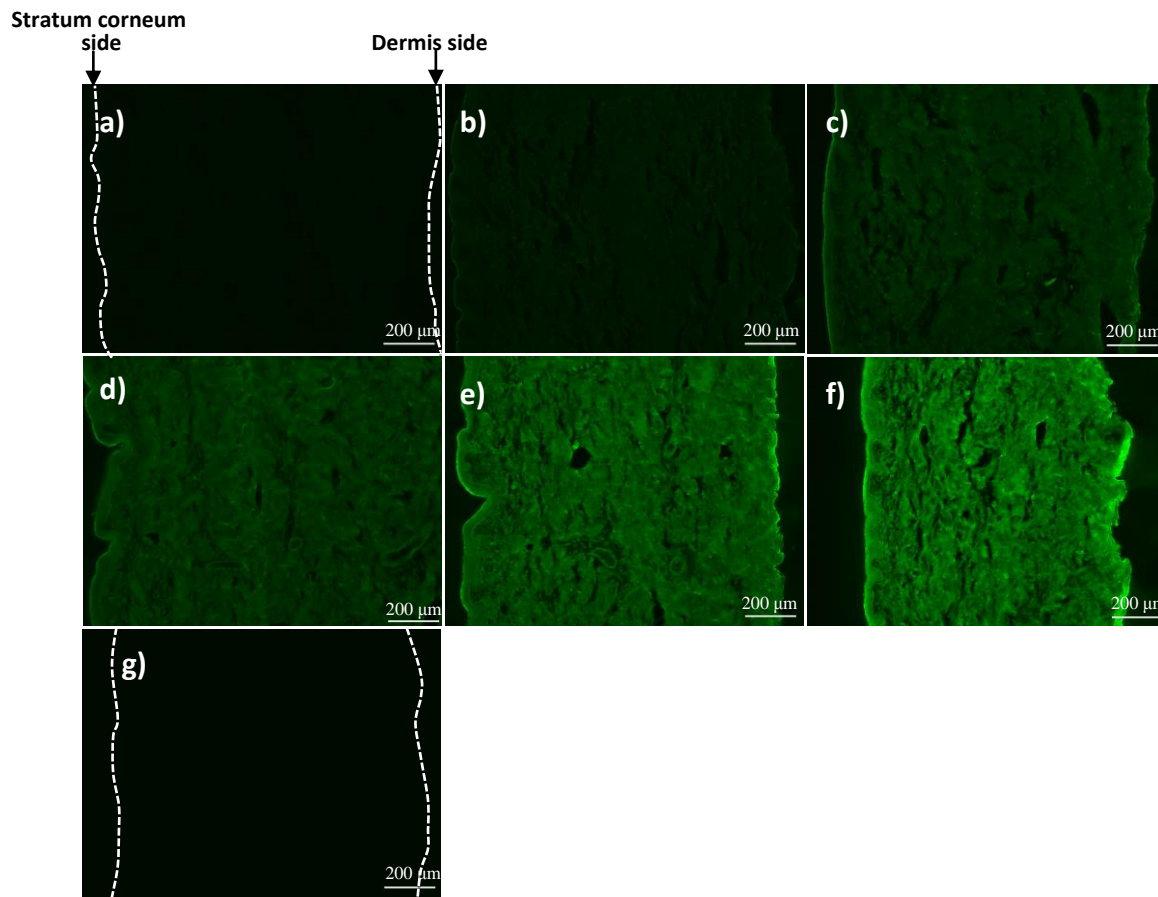
Figure 5. CLSM images for FD-4 fluorescence intensity in stripped pig ear skin after immersions in solutions with different concentrations of FD-4. a) 0.05 mM (0.18 mg/mL), b) 0.5 mM (1.83 mg/mL), c) 1 mM (3.67 µg/mL), d) 2.5 mM (9.17 mg/mL), e) 4 mM (14.68 mg/mL), f) 5 mM (18.35 mg/mL), g) 0 mM (control). Dashed line: boundary of the skin

$$y = 0.0745x + 5.9233$$
$$R^2 = 0.99636$$
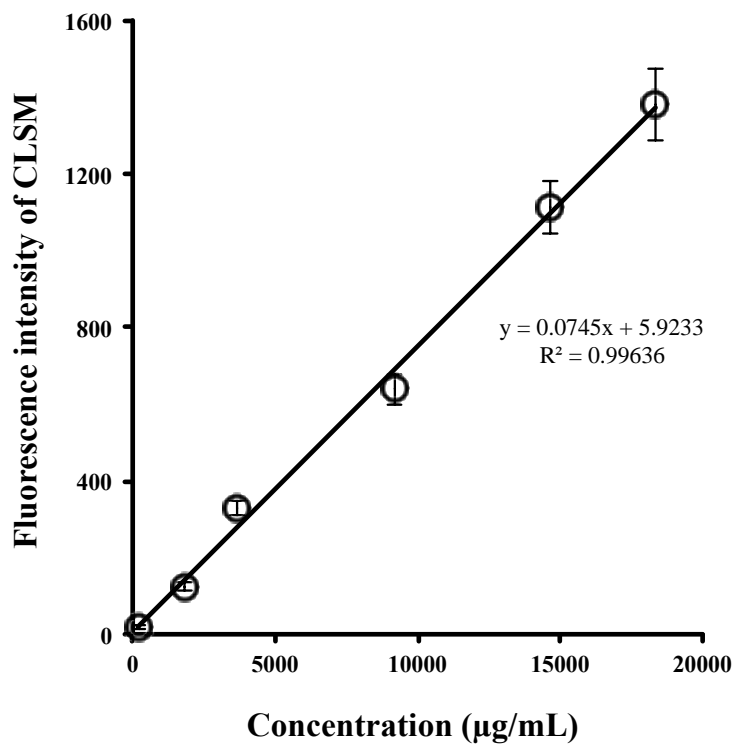
Figure 6. Relationship between FD-4 fluorescence intensity observed by CLSM and the concentration of FD-4 applied. Each point shows the mean ± S.D. (n = 50)
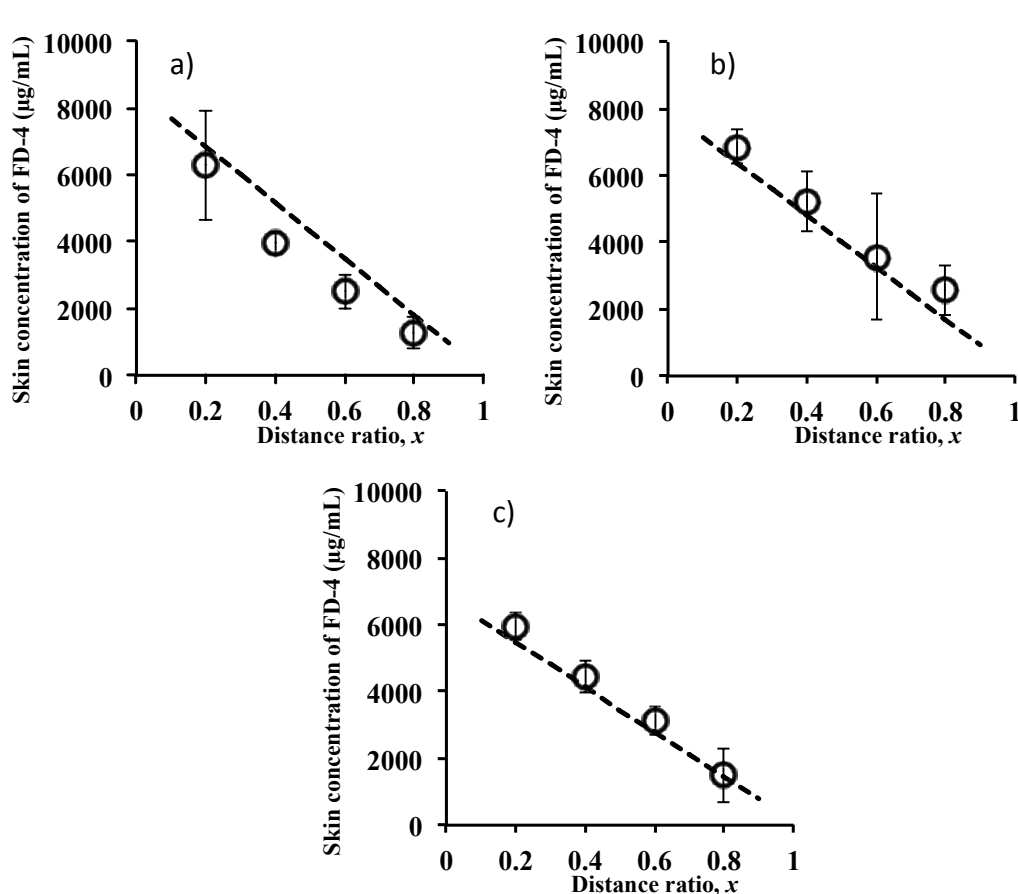
Skin permeation and concentration-distance profiles under the infinite condition

An in vitro skin permeation experiment was performed to further examine the permeation of FD-4 through stripped pig ear skin. Skin permeation experiment was performed in three replicates. Figure 7 shows the time course of the cumulative amount of three individual profiles after topical application of 5 mM FD-4 to the stripped pig ear skin. A typical lag time and subsequent steady state skin permeation were obtained. Furthermore, the profiles obtained in three samples were similar. The concentration-distance profile in the steady state period (5 h after starting the permeation experiment) was determined by the permeation parameters of FD-4 from skin permeation profiles using the difference equation based on the Fick's 2nd law of diffusion as shown in the Methods in the subsection Theoretical (2). The calculated results are shown as dashed lines in Figure 8.
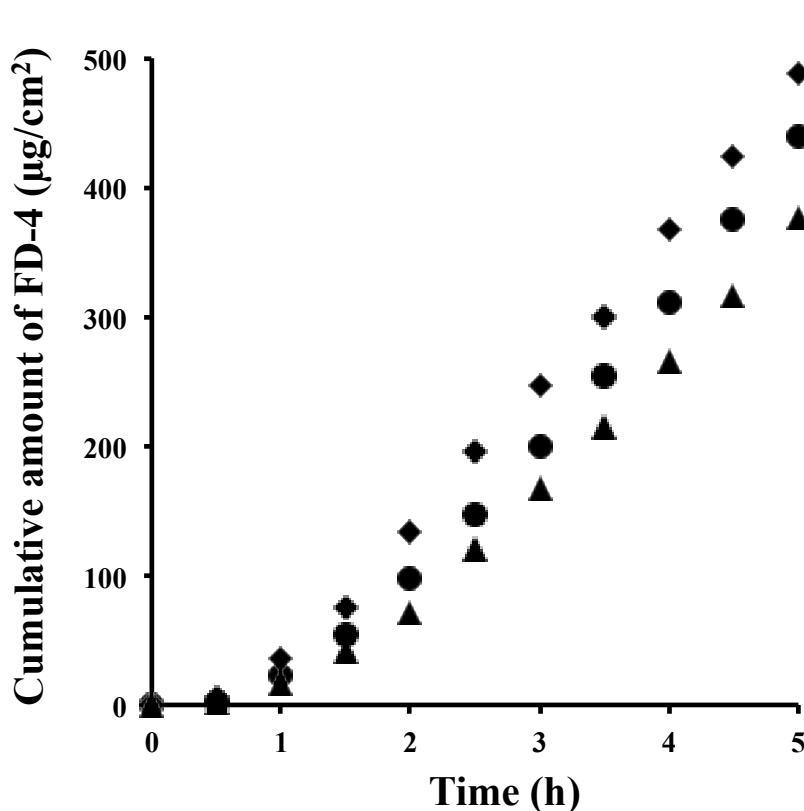

Figure 7. Time course of the cumulative amount of FD-4 that permeated through stripped pig ear skin. ●: sample A, ◆: sample B, ▲: sample C

Two samples were selected from the time courses of the cumulative amounts of FD-4 that permeated through the skin in order to investigate the skin concentration-distance profile of FD-4 in a non-steady state (lag time period). Dashed lines in Figure 9 show the concentration-distance profile obtained in the non-steady state (0.5 h), and these were calculated using the skin permeation parameters obtained from the permeation profile results in Figure 7. The results shown by the dashed lines in Figures 8 and 9 suggested that the concentration-distance profiles of FD-4 in the stripped skin in the steady-state and before the steady-state could be determined from its permeation profiles using the difference equation based on the Fick's law.

Figure 8. Concentration-distance profile of FD-4 in the steady state (5 h). Symbols (○): Observed values from image analysis, Dashed line: Calculated value by the difference equation based on Fick's law of diffusion from the skin permeation profile. Each point shows the mean ± S.D. (n = 4). a), b) and c) correspond to samples A, B and C, respectively
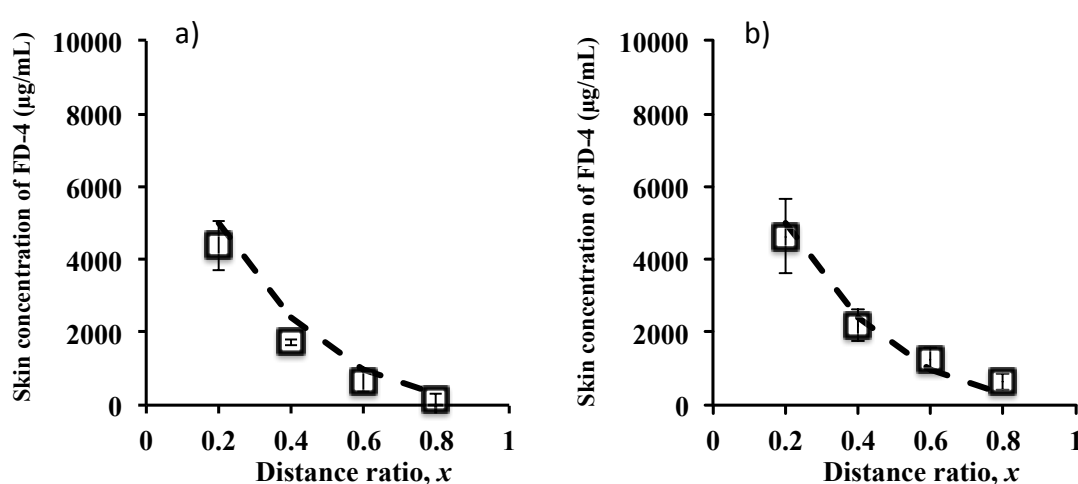
Figure 9. Concentration-distance profile of FD-4 in the non-steady state (0.5). Symbols (□): Observed value from image analysis, Dashed line: Calculated value by the difference equation based on Fick's law of diffusion from the skin permeation profile. Each point shows the mean ± S.D. (n = 4). a) and b) correspond to samples A and B, respectively

Imaging analysis by CLSM and comparison of concentration-distance profiles between observed and calculated values
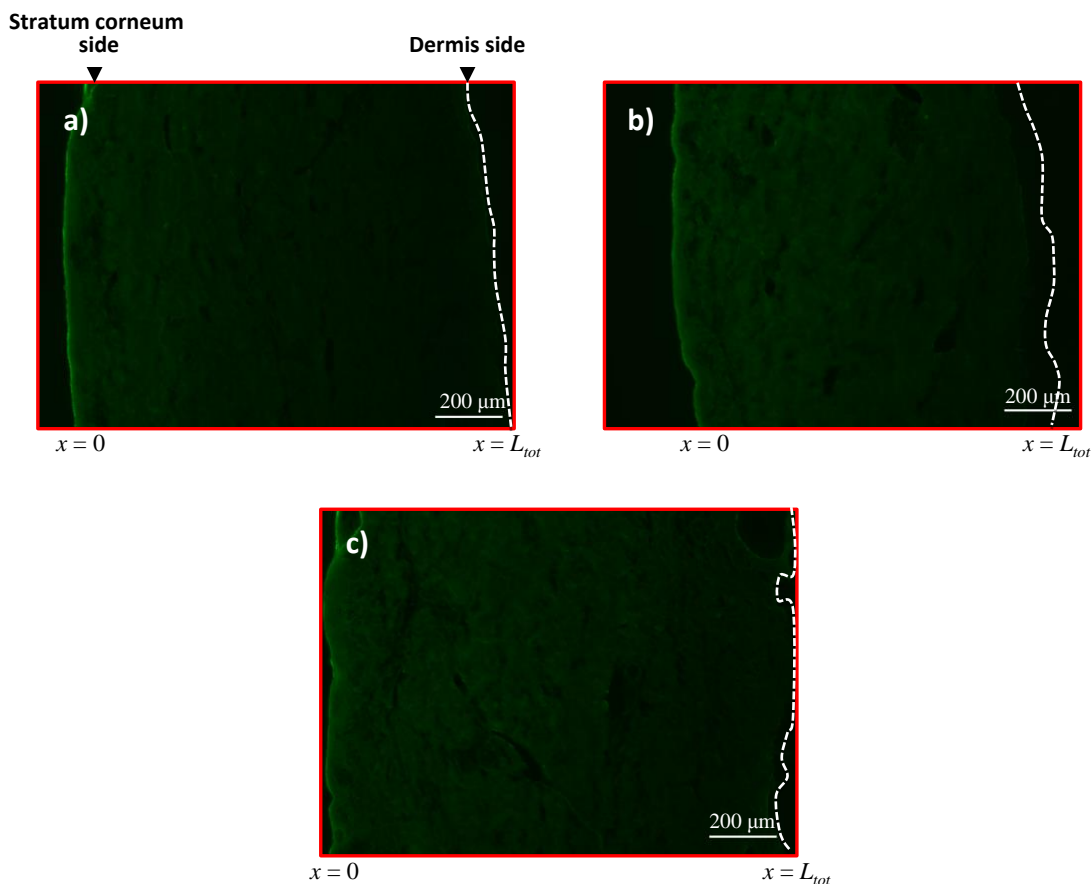
The intensity of fluorescence in the skin was measured by CLSM 0.5 and 5 h after starting the in vitro skin permeation experiment. Figures 10 and 11 show the images obtained of skin sections for the distribution of FD-4 5 and 0.5 h after the skin permeation experiment (in the steady and non-steady states, respectively). The intensity of fluorescence for FD-4 on the applied surface of the stripped pig ear skin was markedly high, while that at the receiver surface was unstable; therefore, it was difficult to quantify the intensity of fluorescence in these two surfaces. These surface intensities were subsequently omitted from the fluorescence analysis. Two images were randomly selected from the time courses of the cumulative amounts of FD-4.

The concentration-distance profiles for FD-4 in the steady state (5 h) and non-steady state (0.5 h) were obtained from image analysis data by CLSM. Each point in Figures 8 and 9 shows the concentration of FD-4 determined by CLSM imaging. The dashed lines in these figures were determined by skin permeation data, as described in (4. 3). The results obtained by CLSM were similar to those from the mathematical approach. These fluorescent gradients due to the permeation of FD-4 across the skin in both the steady state (5 h) and non-steady state (0.5 h) may be useful for visually understanding the concentration-distance profiles of chemical compounds across the skin.

Discussion

We used CLSM to quantitatively determine the skin concentration-distance profile of FD-4 at different depths through stripped skin. Limitations have been associated with the conventional methods used to determine drug concentration-distance profiles in the skin. CLSM could overcome these limitations because it generates high-resolution and sensitive images at multiple depths through the skin without the need for mechanical skin sections after the topical application of fluorescent drugs [29]. We applied a well-established mathematical approach represented by the difference method based on Fick's law of diffusion to obtain the skin concentration-distance profiles of topically applied drugs for comparisons in order to evaluate the present CLSM technique. A strong correlation ($R^2=0.99636$) was observed between the intensity of fluorescence on CLSM images and the applied concentration of FD-4 (Fig. 6), which indicated that the intensity of fluorescence at each depth of the skin could be quantitatively evaluated by CLSM.

Although few studies have determined the drug concentration-distance profiles of topically applied drugs, even less attention has been given to understanding the disposition behavior of these drugs through the skin under both steady-state and non-steady state conditions. Therefore, evaluating skin concentration-distance profiles is important under these conditions in order to address not only to efficacy, but also toxicological issues.

Figure 10. CLSM images of FD-4 fluorescence intensity in stripped pig ear skin in the steady state (5 h) after the permeation experiment. a), b) and c) show samples A, B and C, respectively. Dashed line: boundary of the skin
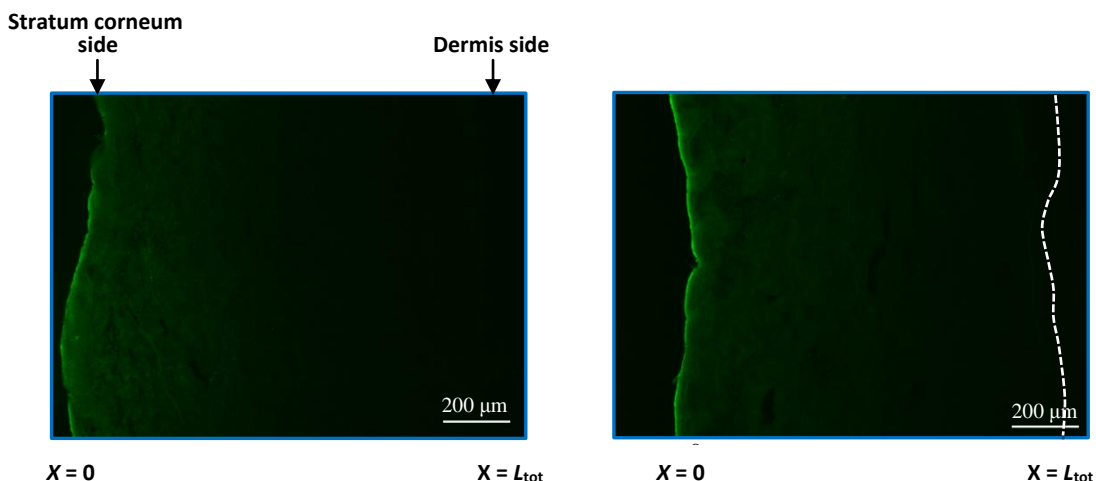
Figure 11. CLSM images of FD-4 fluorescence intensity stripped pig ear skin in the non-steady state (0.5 h) after the permeation experiment. a) and b) show samples A and B, respectively. Dashed line: boundary of the skin

Theoretical and observed FD-4 skin concentration-distance profiles were determined in both the steady and non-steady states in the present study. The theoretical and observed FD-4 concentration-distance profiles were almost equal at the steady and non-steady states (Figs. 8 and 9), which suggested that the concentration of the fluorescence compound may be precisely evaluated at multiple depths through skin using CLSM. Common artifacts include tearing, ripping, holes, and folding may occur during skin sectioning;

therefore, analysis points must be plotted to avoid such artifacts in order to calculate the fluorescent intensity for FD-4 from one skin section (Fig. 3). This could explain why slightly different skin concentration-distance values were obtained for FD-4 between CLSM and the theoretical values (Figs. 8 and 9). Furthermore, plotted analysis points (25, 31, 37 and 43) (Fig. 3) were not selected as reference points to determine skin concentration-distance profiles due to the high intensity of FD-4 at the epidermis side. Plotted analysis points (30, 36, 42 and 48) (Fig. 3) at the dermis side were also not selected as reference points to determine skin concentration-distance profiles because they overlapped with the receiver compartment, which may lead to unclear images by CLSM. The present CLSM method provided a visual observation of drug distribution at multiple depths through the skin (Figs. 10 and 11) as an additional advantage over the mathematical approach. However, the intensity of fluorescence intensity was markedly high on the epidermis surface. Thus, it is necessary to carefully wash the fluorescence compound that is adsorbed on the skin surface. Further studies are needed to evaluate the distribution of FD-4 in skin sections cut laterally as well as through skin appendages such as hair follicles. We intend to use low molecular-weight fluorescence compounds in future studies.

Conclusions

The results of the present study clearly demonstrated that CLSM may be used to quantitatively determine the concentration-distance profiles of topically applied fluorescent drugs. These results provide a useful insight into dermatopharmacokinetics.

References

[1]   A. Naik, Y.N. Kalia, R.H. Guy, *Pharm. Sci. Technol. Today* **3** (2001) 318-326.

[2]   H. Wosicka, K. Cal, *J. Dermatol. Sci*. **57** (2011) 83-89.

[3]   M.R. Prausnitz, S. Mitragotri, R. Langer, *Drug Discovery* **3** (2004) 115-124.

[4]   T. Oshizaka, H. Todo, K. Sugibayashi, *Yakugaku Zasshi* **132** (2012) 1237-1243.

[5]   G. Cevc, U. Vierl, *J. Control. Release* **141** (2010) 277-299.

[6]   O. Sarheed, Y. Frum, *Int. J. Pharm*. **423** (2012) 179-183.

[7]   M. Tsang, R.H. Guy, *Br. J. Dermatol*. **165** (2010) 954-958.

[8]   U. Kiistala, *J. Invest. Dermatol*. **50** (1968) 129-137.

[9]   C. Surber, K.P. Wilhelm, D. Bermann, H.I. Maibach, *Pharm. Res*. **10** (1993) 1291-1294.

[10]   L.K. Pershing, B.S. Silver, G.G. Krueger, V.P. Shah, J.P. Skelley, *Pharm. Res*. **9** (1992) 45-51.

[11]   A. Rougier, D. Dupuis, C. Lotte, R. Roguet, H. Schaefer, *J. Invest. Dermatol*. **81** (1983) 275-278.

[12]   V.P. Shah, G.L. Flynn, A. Yacobi, H.I. Maibach, C. Bon, N.M. Fleischer, T.J. Franz, S.A. Kaplan, J. Kawamoto, L.J. Lesko, J.P. Marty, L.K. Pershing, H. Schaefer, J.A. Sequeira, S.P. Shrivastava, J. Wilkin, R.L. Williams, *Pharm. Res*. **15** (1998) 167-171.

[13]   M. Lodén, L. Ungerth, J. Serup, *Acta Derm. Venereol*. **87** (2007) 485-492.

[14]   B. N'Dri-Stempfer, W.C. Navidi, R.H. Guy, A.L. Bunge, *Pharm. Res*. **26** (2009) 316-328.

[15]   J.E. Rim, P.M. Pinsky, W.W. van Osdol, *J. Membr. Sci*. **20** (2007) 174-182.

[16]   B.D. Weinberg, E. Blanco, J. Gao, *J. Pharm. Sci*. **97** (2008) 1681-1702.

[17]   Y.G. Anissimov, M.S. Roberts, *Pharm. Res*. **28** (2011) 2119-2129.

[18]   L. Hu, M.G. Wientjes, J. Li, J.L. Au, *AAPS J*. **12** (2010) 586-591.

[19]   K. Sugibayashi, H. Todo, T. Oshizaka, Y. Owada, *Pharm. Res*. **27** (2010) 134-142.

[20]   H. Ishii, H. Todo, K. Sugibayashi, *Chem. Pharm. Bull*. **58** (2010) 556-561.

[21]   H. Ishii, K. Fujino, H. Todo, K. Sugibayashi, *Exp. Anim*. **61** (2012) 147-156.

[22] N. Hada, T. Hasegawa, H. Takahashi, T. Ishibashi, K. Sugibayashi, *J. Control. Release* **108** (2005) 341-350.

[23] S. Geinoz, S. Rey, G. Boss, A.L. Bunge, R.H. Guy, P.A. Carrupt, M. Reist, B. Testa, *Pharm. Res*. **19** (2002) 1622-1629.

[24] K. Sato, N. Mitsui, T. Hasegawa, K. Sugibayashi, Y. Morimoto, *J. Control. Release* **73** (2001) 269-277.

[25] K. Sugibayashi, T. Hayashi, K. Matsumoto, T. Hasegawa, *Drug Metab. Pharmacokinet*. **19** (2004) 352-362.

[26] R.J. Scheuplein, I.H. Blank, *J. Invest. Dermatol*. **60** (1973) 286-296.

[27] K. Sugibayashi, T. Hayashi, T. Hatanaka, M. Ogihara, Y. Morimoto, *Pharm. Res*. **13** (1996) 855-860.

[28] H. Takeuchi, M. Ishida, A. Furuya, H. Todo, H. Urano, K. Sugibayashi, *Biol. Pharm. Bull*. **32** (2012) 192-202.

[29] R. Alvarez-Román, A. Naik, Y.N. Kalia, H. Fessia, R.H. Guy, *Eur. J. Pharm. Biopharm*. **58** (2004) 301-316.